Chemical Science

ROYAL SOCIETY OF CHEMISTRY

EDGE ARTICLE

View Article Online
View Journal | View Issue

Cite this: *Chem. Sci.*, 2025, **16**, 16970

All publication charges for this article have been paid for by the Royal Society of Chemistry

Received 5th August 2025
Accepted 19th August 2025

DOI: 10.1039/d5sc05902j

rsc.li/chemical-science

The 'ins' and 'outs' of amidines in β-sheet folding and fibril disaggregation

Emily A. O'Brien, Mohaddeseh Abbasi, Jeffrey A. Purslow and Brett VanVeller *

Amidines are a relatively unexplored isostere of the amide bond, offering unique electronic properties and hydrogen-bonding behavior. This study presents the first systematic investigation of amidines within folded β-sheet structures. Using CD, NMR, and aggregation assays, we find that amidines are well tolerated when acting as hydrogen-bond donors but disrupt β-sheet folding when serving as hydrogen-bond acceptors. This donor/acceptor asymmetry contrasts with the behavior of amidines in α-helices, where both roles are accommodated. Importantly, outward-facing amidines disrupt the edge-to-edge hydrogen bonding required for fibril formation, enabling the design of non-aggregating β-hairpin peptidomimetics without reliance on sequence charge. Spectroscopic analysis further reveals that amidines embedded in peptide backbones exist predominantly in their neutral, monoprotonated form even at acidic pH, prompting a reassessment of amidine basicity in structured biomolecules. These findings establish design principles for using amidines in stable, aggregation-resistant peptidomimetic scaffolds.

1 Introduction

Biosynthetic pathways that modify the main-chain amide bond of peptide natural products imply that such alterations contribute advantageous properties compared to native amide bonds.[1–8] While the synthetic alteration of amino-acid side-chain structures and functional groups through mutagenesis has been a mainstay in peptide design,[9] backbone modifications are a comparatively untapped opportunity, despite the fact that backbone interactions are primarily responsible for dictating peptide folding and secondary structure. Although various motifs have been explored as alternatives to the amide bond in β-sheets,[10–13] the amidine is a particular peptide-bond isostere that has not been considered in folded β-sheet structure and has received considerably little attention in peptides more generally.[14,15]

Amidines differ from conventional peptide bonds by a single atom swap of the carbonyl oxygen for a nitrogen,[16–18] and have served as design elements in pharmaceutical compounds.[19–25] Specifically, Boger and coworkers have proposed that the different protic states of the amidine are responsible for the ability of vancomycin derivatives containing amidines (so-called maxamycins) to target antibiotic resistant Gram-positive bacteria.[26–30] Amidines are also present in a class of natural products known as ribosomally synthesized and post-translationally modified peptides (RiPPs), which implies that an evolutionary advantage may have driven the development of biosynthetic mechanisms for their incorporation.[1–3] Additionally, amidines have been proposed as potential intermediates in the prebiotic formation of peptides.[31–33] Despite these examples from nature, there is a dearth of studies investigating amidines within synthetic peptides,[14,15,34] which likely derives from a historical lack of robust methods for their incorporation into peptides.

Our initial report of a general methods to site-selectively install amidines in place of traditional peptide bonds[35] created the first opportunity to explore the impact of this amide-bond isostere in α-helical structure.[14] We found that amidines displayed intuitive hydrogen-bonding interactions that responded to pH and were amenable to design. The greater basicity of the amidine nitrogen led to stronger hydrogen-bond acceptor interactions that increased the stability and extent of helical folding. Ultimately, amidines appeared to be one of the

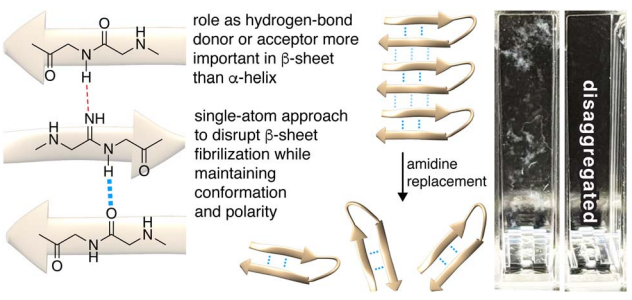

Fig. 1 Hydrogen-bonding interactions of amidines in folded peptide secondary structure and effect on β-fibril aggregation.

Department of Chemistry, Iowa State University, Ames, IA, 50011, USA. E-mail: bvv@iastate.edu

few isosteric mimics of amides that could stabilize helical structure as both a hydrogen-bond donor and an acceptor.[18]

This work marks the first systematic investigation of amidines within folded β-sheet structures (Fig. 1). Amidines are a relatively unexplored single-atom isostere of the amide bond, offering unique electronic properties and hydrogen-bonding behavior. Using CD, NMR, and aggregation assays, we find that amidines are well tolerated in β-sheets when acting as hydrogen-bond donors, but disrupt folding when serving as acceptors. This donor/acceptor asymmetry contrasts with their behavior in α-helices, where both roles are accommodated. Outward-facing amidines further prevent fibril formation by disrupting the edge-to-edge hydrogen bonds required for self-association, enabling the design of non-aggregating β-hairpin peptidomimetics without reliance on sequence charge. Spectroscopic analysis reveals that amidines embedded in peptide backbones exist predominantly in a neutral, monoprotonated state even at acidic pH. Taken together, these findings position amidines as minimal, modular elements for engineering stable, aggregation-resistant peptidomimetic scaffolds—closely approximating native amides in conformation and polarity, unlike *N*-methyl amides or thioamides, which respectively distort geometry or increase hydrophobicity.

2 Results and discussion

To begin the investigation of how amidines might behave within β-sheet structure, we chose to study a model β-hairpin peptide originally developed by Gellman and coworkers dubbed YKL (Table 1).[36,37] This peptide has been used in a variety of studies to investigate the effect of backbone modifications on folded structure, including aza-peptides,[10] thioamides,[11,12] and *N*-methylated amides,[13] providing an excellent test bed for comparisons to amidine behavior.

With the native YKL sequence serving as a starting control, we synthesized[35] six amidinopeptide analogues, featuring an amidine at different positions along the strand, both distal and proximal to the turn (Table 1). The positions of the amidine were selected to represent equal opportunities for the amidine to either point 'out' of the β-hairpin and into solution or point 'in' to the seam of hydrogen bonds that knit the β-hairpin together. Finally, we synthesized **7**, which was assumed to be completely unfolded,[10,12] through substitution of the turn-stabilizing D-Pro$_6$ residue with L-Pro$_6$. Closure of the β-hairpin into a cyclic peptide through inclusion of another D-Pro-Gly motif provided **8**, which was assumed to be completely folded (Table 1).[10] These peptides served as additional controls to quantify the extent of folding (*vide infra*).

2.1 Characterization of β-hairpin structure by circular dichroism

The circular dichroism (CD) spectrum of the YKL control peptide exhibited a characteristic single minimum at 215 nm, which is indicative of anti-parallel β-sheet structure. An obvious dichotomy was observed for the amidinopeptides under consideration in this study. Specifically, all peptides for which the amidine ^{2}*N*-imino moiety pointed 'out' of the β-hairpin and into solution displayed similar minima around 215 nm, signifying β-sheet character (**1**-Tyr$_2^{(NH)}$, **3**-Glu$_4^{(NH)}$, **4**-Gly$_7^{(NH)}$, Fig. 2A). Alternatively, all peptides for which the amidine ^{2}*N*-imino moiety pointed 'in' to the β-hairpin did not display any signatures that are characteristic of well-folded peptide structure (**2**-Val$_3^{(NH)}$, **5**-Orn$_8^{NH}$, **6**-Ile$_{10}^{(NH)}$, Fig. 2B).

Table 1 Structure of amidinopeptides and folded controls

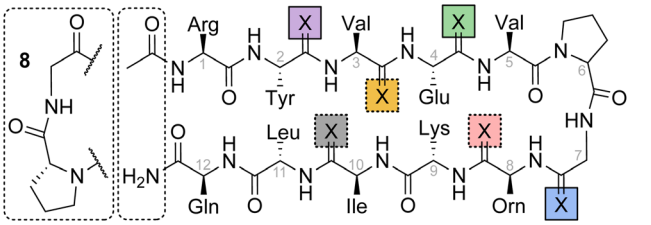

	Amidine	sequence[a]		
Peptide	Orientation	Strand	Turn	Strand
YKL		RYVEV	pG	OKILQ
1-Tyr$_2^{(NH)}$	'Out'	RY$^{(NH)}$VEV	pG	OKILQ
2-Val$_3^{(NH)}$	'In'	RYV$^{(NH)}$EV	pG	OKILQ
3-Glu$_4^{(NH)}$	'Out'	RYVE$^{(NH)}$V	pG	OKILQ
4-Gly$_7^{(NH)}$	'Out'	RYVEV	pG$^{(NH)}$	OKILQ
5-Orn$_8^{(NH)}$	'In'	RYVEV	pG	O$^{(NH)}$KILQ
6-Ile$_{10}^{(NH)}$	'In'	RYVEV	pG	OKI$^{(NH)}$LQ
7		RYVEV	PG	OKILQ
8[b]		RYVEV	pG	OKILQpG
		cyclic		

[a] All peptides except **8** are capped at the N-terminus with Ac and have a C-terminal amide (–CONH$_2$). [b] Head-to-tail cyclic peptide.

2.2 Characterization of β-hairpin conformation *via* NMR

To further interrogate the results of the CD experiments and the secondary structures of the amidinopeptides under consideration, we used 2-dimensional NMR experiments. First, ^{13}C–^{1}H and ^{15}N–^{1}H HQSC, NOESY, and TOCSY experiments were used to fully assign the chemical shifts of the amidinopeptide β-hairpins (see Tables S2 and S3 in SI for residue assignments).

The chemical shift assignments allowed us to estimate the nature of the folded structure for each residue (Fig. 2C). The difference between the $^{13}C^{\alpha}$ and $^{13}C^{\beta}$ chemical shifts has been shown to be an accurate and sensitive indicator of secondary structure, and even more accurate than H^{α} chemical shifts when distinguishing an β-sheet from a random coil.[38–40] Specifically, compared to a random coil, negative $\Delta\delta C^{\alpha}$–$\Delta\delta C^{\beta}$ values are indicative of β-sheet structure (where positive $\Delta\delta C^{\alpha}$–$\Delta\delta C^{\beta}$ values indicate α-helical structure).[41–43]

The same dichotomy that was observed for the CD results was observed for the secondary structure analysis by NMR (Fig. 2C). All peptides for which the amidine pointed 'out' of the proposed β-hairpin fold generally displayed negative $\Delta\delta C^{\alpha}$–

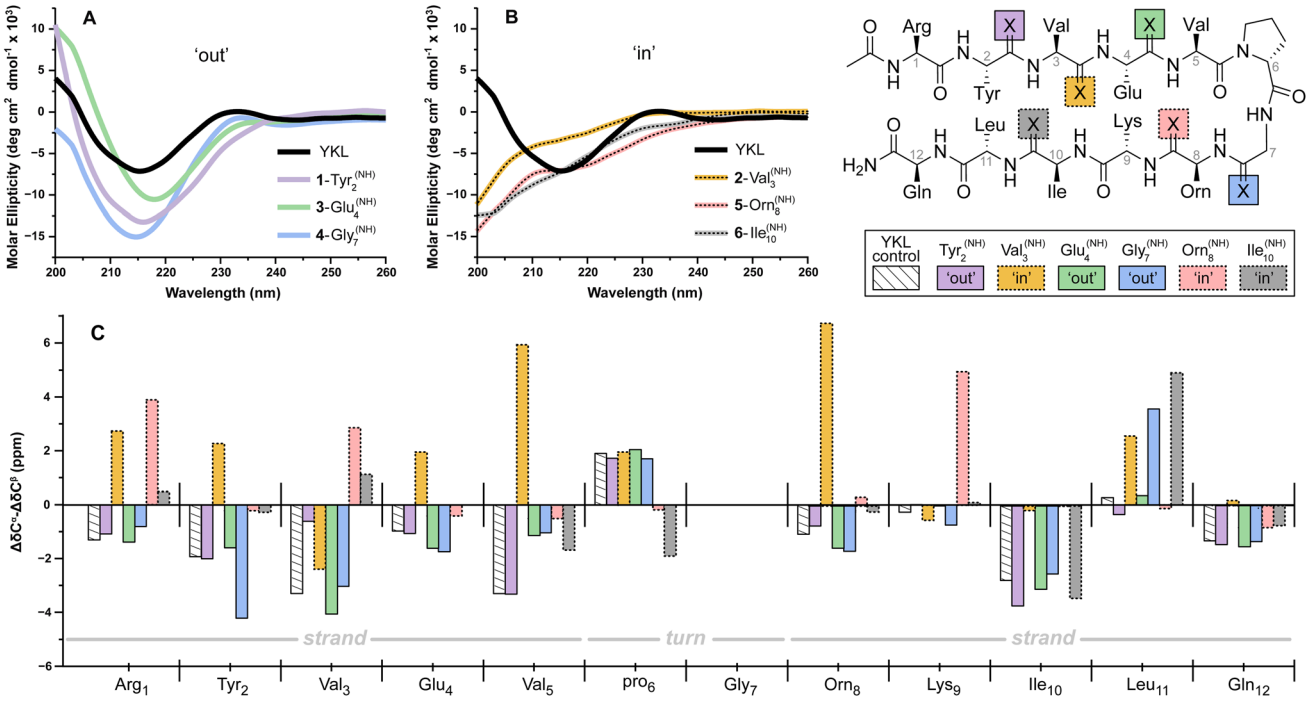

Fig. 2 Characterization of β-hairpin structure and conformation of peptides at 20 °C in sodium acetate buffer at pH 4.0. (A) and (B) Circular dichroism. (C) Secondary structure analysis using the difference between experimentally observed and theoretical values of random $^{13}C^{\alpha}$ and $^{13}C^{\beta}$ chemical shifts. Negative $\Delta\delta C^{\alpha}-\Delta\delta C^{\beta}$ values are indicative of β-sheet structure.

$\Delta\delta C^{\beta}$ values for the residues associated with the β-sheet motifs (*i.e.* residues 1 → 5 and 8 → 12). Alternatively, all peptides for which the amidine pointed 'in' to the β-hairpin fold generally showed variable positive and negative $\Delta\delta C^{\alpha}-\Delta\delta C^{\beta}$ values along the sequence, indicative of greater disorder and a poorly folded β-sheet. Finally, peptides that displayed similar $\Delta\delta C^{\alpha}-\Delta\delta C^{\beta}$ values for their D-Pro residues to that of the YKL control peptide, were interpreted to have similar hairpin turn structure.

Further evidence for the folded β-hairpin fold was provided by the through-space interactions (NOEs) between residues across the β-strands, which are indicated in Fig. 3.[44] This analysis was only carried out for the 'out' peptides which showed well-behaved folding by CD and chemical shift assignment (Fig. 2). Key signatures in the $^{1}H-^{1}H$ NOE spectra are the correlation between the amide proton (NH) and the C^{α}–H proton signals of residues across the strand,[45] in addition to through-space interactions between side-chain atoms that should reside on the same side of the β-sheet. Specifically, through-space NOE correlations for the NH of Orn_8 to the NH of Val_5 are a signature of the β-turn motif.[44,45] Many of the correlations that we observed for the YKL control peptide,[44] were observed for the 'out' amidino-β-hairpins, lending further support to the folded structures proposed here. Specifically, through-space NOE correlations were observed for Tyr_2 to Gln_{12} for **1**-$Tyr^{(NH)}$ and **3**-$Glu^{(NH)}$ peptides. These residues are obviously distal to one another along the sequence, but their spacial proximity is strong evidence of β-hairpin folding. Interestingly, we observed fewer cross strand interactions for peptide **4**-

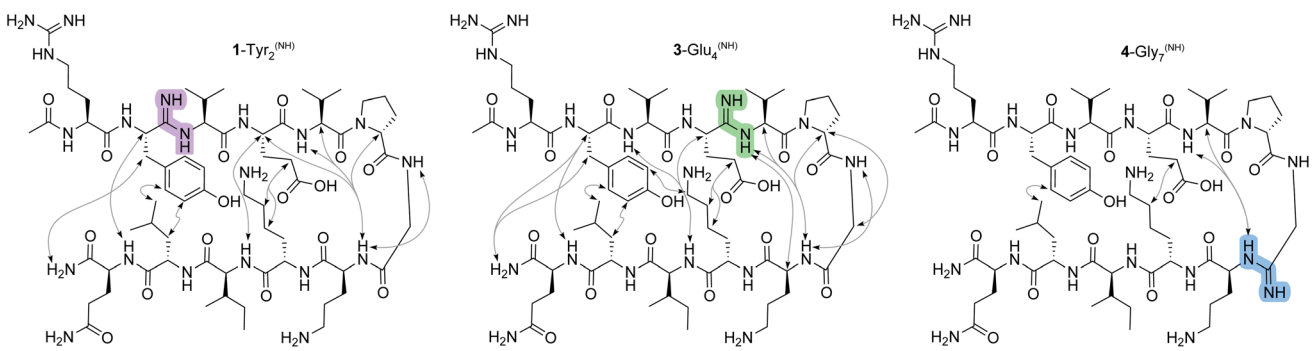

Fig. 3 Observed and spectrally-resolved through space interactions of folded amidinopeptides **1**-$Tyr_2^{(NH)}$, **3**-$Glu_4^{(NH)}$, and **4**-$Gly_7^{(NH)}$ derived from $^{1}H-^{1}H$ NOE experiments.

$Gly_7^{(NH)}$ compared to the other two 'out' amidino-β-hairpins, despite separate evidence suggesting it does adopt a robust β-hairpin (*vide infra*).

2.3 Quantification of folding and stability

This is the first study to characterize the behavior of amidines in β-sheet structure. Thus, we sought to gain a more quantitative understanding of how the amidine impacted the extent of folding and the stability of the β-hairpin structures. We utilized two different methods to determine the fraction of folded peptide at equilibrium, where each method examined different aspects of chemical shift differences relative to control peptides that were considered to be either fully folded (100%) or fully unfolded (0%). Specifically, we chose peptide **8**, a well-characterized cyclic amide control, as the 100% folded reference because it exhibits well-established chemical shift markers of β-hairpin structure. While the most rigorous approach would involve synthesizing cyclic amidino analogues for each modified position, the folding behavior of such peptides cannot be assumed and might not provide a reliable benchmark. Moreover, we used chemical shift markers that are distal from the site of amidine incorporation to minimize localized perturbations and ensure meaningful comparison to the amide reference.

The first method examined the chemical shifts of the Gly_7 diastereotopic H^{α} protons (eqn (1)).[10,12,46,47] Where $\Delta\delta Gly_7$ was the chemical shift difference between the two H^{α} protons for the Gly_7 residue in the peptides under consideration (**1–6**) relative to the same value ($\Delta\delta Gly_7$(**8**)) for the cyclic control peptide (**8**), which was considered to be 100% folded. The closer eqn (1) was to unity, the closer amidino peptides **1–6** were considered to be folded into a β-hairpin (Table 2).

$$\text{Fraction folded}(f) = \frac{\Delta\delta Gly_7(\mathbf{1-6})}{\Delta\delta Gly_7(\mathbf{8})} \quad (1)$$

$$\text{Fraction folded} = \frac{\delta_{\mathbf{1-6}} - \delta_{\mathbf{7}}}{\delta_{\mathbf{8}} - \delta_{\mathbf{7}}} \Big\} \text{for } Val_3,\ Orn_8,\ Ile_{10} \quad (2)$$

The second method considered the chemical shift of the H^{α} protons for residues Val_3, Orn_8, and Ile_{11} to be diagnostic of the fraction folded.[10,12,46,47] To assess the extent of folding, the H^{α} chemical shift for those residues in amidinopeptides (**1–6**) were related to those same chemical shifts in both the unfolded (**7**) and folded (**8**) control peptides (eqn (2)). Again, the closer that eqn (2) was to unity, the more peptides **1–6** were considered to be folded into a β-hairpin (Table 2).

The results from both of these analyses confirm the CD and NMR characterization data discussed above (Table 2). All peptides for which the amidine pointed 'out' of the β-sheet displayed folding values on par with the YKL control peptide, while all 'in' peptides display much lower degrees of folding relative to the control. It should be noted that eqn (1) can overestimate the fraction folded;[10,48] however, the values for eqn (2) provide confirmatory metrics that collectively indicate that amidines are fully tolerated as isosteric replacements of amide bonds in β-sheets, provided the amidine points 'out' and away of the seam of hydrogen bonds necessary to stitch the β-strands together. Alternatively, the amidine at residues Val_3, Orn_8, and Ile_{10} alters the chemical shift of the H^{α} away from standard values used in the development of eqn (2).[14] However, eqn (1) compensates for this limitation by examining Gly_7 residues instead of the amidine-containing residue, lending confidence to the conclusions of this analysis.

Table 2 Fraction folded β-hairpin derived from characteristic NMR features. Values in the structure below are an average of eqn (1) and (2)

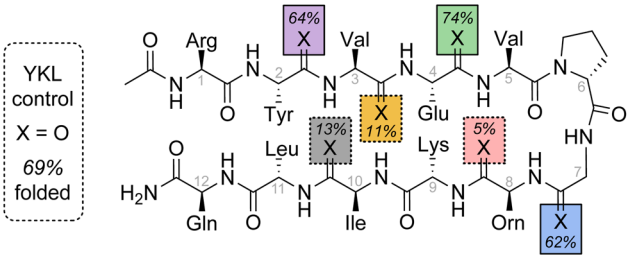

Peptide	Amidine	Eqn (1)	Eqn (2)[a] Val_3	Eqn (2)[a] Orn_8	Eqn (2)[a] Ile_{10}
YKL		0.85	0.59	0.84	0.49
1-$Tyr_2^{(NH)}$	'Out'	0.82	0.42	0.73	0.60
2-$Val_3^{(NH)}$	'In'	0.30		0.02	0.01
3-$Glu_4^{(NH)}$	'Out'	0.96	0.72	0.93	0.36
4-$Gly_7^{(NH)}$	'Out'	0.61	0.61	0.81	0.48
5-$Orn_8^{(NH)}$	'In'	0.03	0.03		0.08
6-$Ile_{10}^{(NH)}$	'In'	0.16	0.03	0.19	

[a] Blank entries in the table correspond to peptides for which the amidine at those residues (Val_3, Orn_8, Ile_{10}) affected the chemical shift of the H^{α},[14] making it irrelevant for analysis. Each folded % in the structure above the table corresponds to an X = NH at that position while keeping amides (X = O) at the other positions along the backbone, and is an average of the calculated values of fraction folded (eqn (1), Val_3, Orn_8, Ile_{10}) for that peptide.

2.3.1 Variable temperature NMR and folding stability. Eqn (1) was also used to analyze the fraction folded as the temperature was increased from 10 °C to 70 °C, to estimate the stability of each peptide ($\Delta G_{folding}$, Table S5). In general, we found that the β-hairpins for which the amidine pointed 'out' of the β-strand (**1**-$Tyr_2^{(NH)}$, **3**-$Glu_4^{(NH)}$, and **4**-$Gly_7^{(NH)}$) exhibited nearly identical $\Delta G_{folding}$ to the YKL control peptide (Table S5). Additionally, we compared the changes in chemical shift of the backbone amide protons with respect to temperature for all peptides (in ppb K^{-1}, Fig. S7 and Table S6). Again, these changes were similar for **1**-$Tyr_2^{(NH)}$, **3**-$Glu_4^{(NH)}$, **4**-$Gly_7^{(NH)}$, and YKL control but different for the unfolded peptide **2**-$Val_3^{(NH)}$, particularly for residues that participate in cross-strand, hydrogen-bonding interactions (See SI for further discussion of individual residue behavior).[49] The collective results of these studies further confirm that the amidine can replicate the behavior of amides in hydrogen-bond donating positions with minimal perturbation to the folded structure.

2.4 Geometric constraints of amidines in β-sheets

We hypothesize that disruption of the β-hairpin by amidines pointing 'in' to the hydrogen-bonding seam arises from the additional hydrogen atom present on the amidine NH, compared to the carbonyl oxygen of the native amide. The planar structure of the β-sheet hydrogen-bond network results in densely packed structure, leaving little to no spatial allowance for the extra NH group. This steric and electronic congestion likely distorts the geometry and disrupts interstrand hydrogen bonding.

In contrast, amidines are tolerated as hydrogen-bond acceptors in α-helices, where the helical curvature allows the extra N–H bond to project outward into solvent (Fig. S44). This structural flexibility helps accommodate the amidine without compromising the fold.[14] Supporting this interpretation, previous studies have shown that α-helices are more tolerant to side-chain mutations than β-sheets due to their cylindrical geometry and greater conformational plasticity.[50] Moreover, the hydrogen bonds in β-sheets are stronger, more linear and tightly packed than those in α-helices,[51] which may make them less tolerant to perturbation by amide isosteres. Our findings reinforce these structural distinctions and offer new insight into secondary structure compatibility by probing with amidines as a minimal, backbone-focused perturbation.

While steric crowding from the additional NH group of the amidine likely contributes to destabilization when oriented internally, we cannot exclude the possibility that changes in the hydrogen-bond register or local ϕ/ψ angles also play a role. In particular, the presence of β-branched residues (Val_3, Ile_{10}) at these positions may amplify the conformational strain induced by the amidine. Future computational or mutational studies will be valuable in dissecting these effects in more detail.

2.5 Protic state of the amidine in β-sheet structure

To estimate the protic state of the amidine, we exploited our synthetic approach[35,52] to install a spin $\frac{1}{2}$ ^{15}N nucleus at the ^{2}N-imino position of the amidine in **1**-$Tyr_2^{(NH)}$. Interrogation of the amidine protic state through ^{15}N–^{1}H HSQC experiments was carried out in sodium acetate buffer at pH 4 to limit loss of signal due to fast-exchange processes with solvent (Fig. 4A–D).

At 20 °C, we observed a strong peak for the amidine in **1**-$Tyr_2^{(NH)}$ due to the isotopic enrichment (Fig. 4A). When the ^{15}N decoupling in the indirect dimension was removed, we observed the amidine peak split into a doublet with a $^{1}J_{N-H}$ coupling of 92 Hz (Fig. 4B). The splitting and coupling value are consistent with a singly protonated, neutral =NH species.[53–55] The nearby doublet for the Gly_7 amide NH provided a convenient *in situ* verification of the single protonation, further validating this finding (Fig. 4A). At temperatures above 20 °C, we observed broadening of the amidine signal beyond detection, indicating the amidine is undergoing chemical exchange on the intermediate NMR timescale.

As the temperature was lowered to 10 °C, extensive line broadening of the amidine signal was observed, suggesting the presence of millisecond-timescale conformational transitions

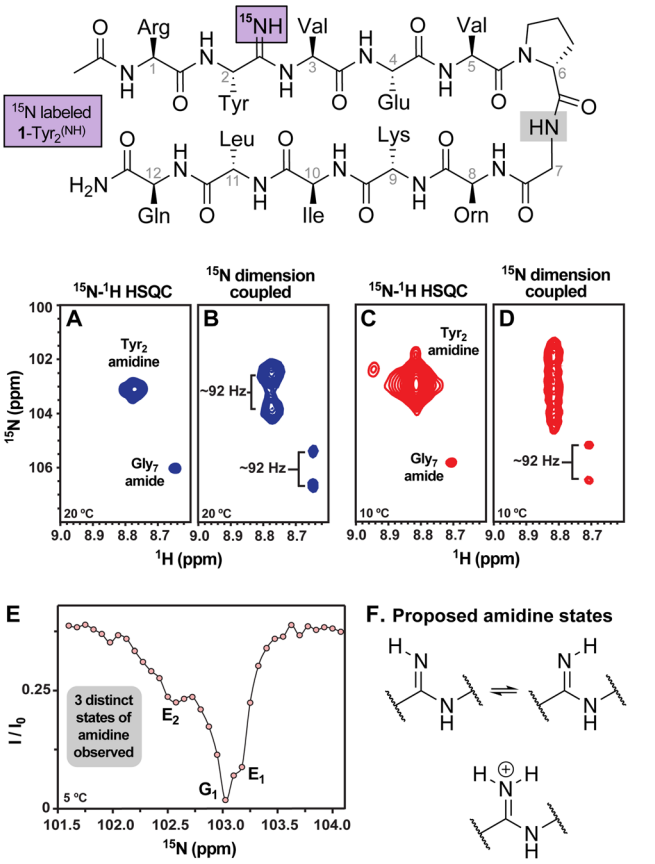

Fig. 4 ^{15}N–^{1}H HSQC and ^{15}N–^{1}H HSQC coupled in the indirect dimension (^{15}N) to reveal $^{1}J_{N-H}$ coupling at 20 °C (A and B) and 10 °C (C and D) at pH 4. (E) ^{15}N Chemical Exchange Saturation Transfer (CEST) profile of the amidine of **1**-$Tyr_2^{(NH)}$. The global minimum corresponds to the major state, G_1, whereas the local minima correspond to energetically excited conformational states, E_1 and E_2. An intensity profile was obtained by quantifying the intensity of the visible-state peak as a function of position of the weak B_1 irradiation field. A spectrum was collected with $B_1 = 6$ Hz every 0.075 ppm from 101 to 104.5 ppm. The ratio I/I_0 is plotted, where I is the intensity after a period of irradiation ($T_{ex} = 0.2$ s). I_0 is the intensity when $T_{ex} = 0$ s. (F) Proposed amidine states from CEST experiments.

and/or the presence of alternate conformational states (Fig. 4C and D).[56] To further probe these states, we performed a ^{15}N Chemical Exchange Saturation Transfer (CEST) experiment (Fig. 4E).[57–59] In CEST, a weak radiofrequency field (B_1) is applied to monitor the magnetization transfer to sites undergoing conformational exchange. We specifically targeted the amidine region (101 to 104.5 ppm) and decreased the temperature to 5 °C to increase signal-to-noise. The global minimum (G_1) in the CEST profile signals the major state. If the global minimum (G_1) is undergoing exchange with alternate states, additional weaker minima (E_{1-2}) equal to the number of detectable alternate states are observed.[58] The results of the CEST experiment revealed that the major populated state of the amidine (G_1) undergoes conformational exchange with two additional minor states (E_1 and E_2) (Fig. 4E). Given the dominance of the singly protonated =NH species at elevated temperature, we speculate that one of these two minor states is the conformational isomer of the

singly protonated amidine (Fig. 4F). The other minor state could be the transient doubly protonated amidinium (Fig. 4F), which is a reasonable proposition given the pH of 4 and basic site present on the amidine. While beyond the scope of this work, these findings compel further experiments to understand the ensemble of states that amidines appear to undergo on the slow-to-intermediate timescale. This observation alone is surprising because the amidine ^{15}N points into bulk solvent, which typically renders these exchanges too fast to detect on the timescale probed by CEST experiments. Such hidden states can be critical for evaluating the mechanism and binding of drug (macro)molecules to their protein targets.

Collectively, these data indicate that the dominant species for the amidine along the β-strand is the neutral monoprotonated state, even at the acidic pH of 4. This result contrasts with traditional views of amidines being highly basic (pK_{aH} ≈ 12), and generally associated with poor pharmacokinetic properties in small molecules.[60–62] However, we have found that amidines within peptide backbones can be considerably less basic (pK_{aH} 5–6),[14] perhaps due to reduced solvation of the amidine when placed within a peptide backbone. Regardless of the explanation, it is clear that amidines are far more tunable in terms of their basicity compared to the related guanidine functional group in the side-chain of arginine. Spectroscopic evidence indicates that arginine side chains are invariably protonated and charged (pK_a > 12) in proteins, even when buried within hydrophobic microenvironments.[63] Amidines do not appear to follow this behavior, however, an evaluation of the physical properties of more structurally diverse amidines is warranted.

2.6 A single-atom approach to mitigate aggregation

The results above outline the impact that amidines have on folded β-sheet structure. Specifically, amidines do not significantly impact the structure of β-sheets as hydrogen-bond donors, but do significantly disrupt β-sheet folding if an amidine is operating as a hydrogen-bond acceptor. These findings led us to hypothesize that amidines could be effective for creating β-hairpin peptidomimetics that do not aggregate *via* self-association. Briefly, β-sheets and β-hairpins are prone to fibrillization through edge-to-edge association of the β-strands, leading to extended sheet structures and aggregation.[64] To address this issue, β-sheet models are often endowed with positive charge to discourage aggregation,[37,47] but this limits the sequence variation and the menu of amino acids that might be employed in such structures. However, β-hairpins featuring amidines pointing 'out' of the fold can inhibit aggregation by selectively disrupting the hydrogen bonds required for edge-to-edge association—without compromising the native conformation of the peptide backbone. This strategy enables greater flexibility in sequence design by decoupling aggregation resistance from charge-based constraints.

To test this hypothesis, we synthesized three more peptides (Table 3). The YKL model peptide sequence contains three positively charged residues (Arg_1, Orn_8, Lys_9) and does not display significant aggregation over extended time periods at the concentrations (4 mM) employed above. This behavior indicates why it has become a valuable model sequence for examining β-sheet behavior.[10–13] We mutated two of the positively charged residues to neutral residues (R1Q, O8T) to give **9**, which has neutral net charge. We observed a characteristic CD signature of β-sheet structure for **9** (Fig. S39, 100 μM), that matched the YKL control and indicated that the removal of charged residues was not detrimental to folding of the β-hairpin. By monitoring the transmittance of a 1 mM solution of **9**, we observed an induction period[65] followed by gelation that signaled aggregation of the peptide (Table 3, these results were confirmed by dynamic light scattering (DLS) experiments, see Fig. S43).

As a control, to probe whether the sequence of **9** was itself responsible for aggregation, we synthesized **10**, which featured an L-Pro_6 in place of the D-Pro_6 in **9**. Because the D-Pro_6 is necessary for β-hairpin formation,[10,12] peptide **10** was observed to be a linear random coil in CD experiments (Fig. S39). Accordingly, we did not observe any change in transmittance of a solution of **10** over the same time frame and concentration as **9** (Table 3 and DLS Fig. S43), indicating that aggregation was due to the β-hairpin structure and edge-to-edge fibrilization of the β-sheets.

Finally, we synthesized analogue **11**-$Tyr_2^{(NH)}$ with an amidine at Tyr_2 pointing 'out' of the β-hairpin (Table 3). We observed characteristic signatures of β-hairpin structure in analogy to **9** by both CD, NMR secondary structure and NOE analysis

Table 3 Sequences to test aggregation hypothesis

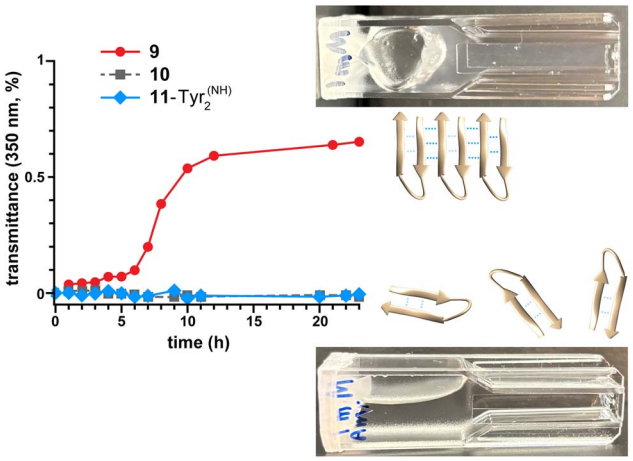

Peptide	Net charge (Side chain)	sequence[a] Strand	Turn	Strand
YKL	+2	RYVEV	pG	OKILQ
9	0	QYVEV	pG	TKILQ
10	0	QYVEV	PG	TKILQ
11-Tyr_2	0	QY$^{(NH)}$VEV	pG	TKILQ

[a] All peptides were capped at the N-terminus with Ac and have a C-terminal amide (–$CONH_2$). Photographic images were captured under ambient light.

(Fig. S37–S39) that allowed us to estimate that **11**-$Tyr_2^{(NH)}$ was folded to the same extent as the other 'out' peptides under consideration (Table 2). In contrast to **9**, however, no aggregation or change in transmittance was observed (and DLS measurements aligned with the monomeric control peptide **10**, Fig. S43). These results support our hypothesis that amidines pointing 'out' of the fold and into solution prevent aggregation by disrupting the hydrogen-bonding interactions necessary for edge-to-edge aggregation.

Together, these findings demonstrate that a single-atom substitution—a strategically positioned amidine in the β-hairpin—can prevent aggregation without compromising fold stability. Outward-facing amidines disrupt the directional hydrogen-bonding network required for edge-to-edge association, enabling a minimalist and modular strategy to inhibit aggregation. Crucially, this approach decouples aggregation resistance from sequence charge, expanding the design space for folded peptidomimetics targeting protein–protein interactions.

3 Conclusion

This work presents the first systematic study of amidines within folded β-sheet structures, establishing their potential as minimal and modular amide isosteres for peptide design. Unlike many other backbone modifications, amidines closely preserve the conformation and polarity of native amides—unlike *N*-methyl amides, which distort folding geometry, or thioamides, which increase hydrophobicity. Our findings reveal that amidines are compatible with β-hairpin structure when acting as hydrogen-bond donors but disrupt folding when positioned as acceptors, highlighting a directional asymmetry not observed in α-helices.

Outward-facing amidines inhibit aggregation by blocking edge-to-edge hydrogen bonding, enabling the design of non-aggregating β-hairpins without introducing net charge. This charge-independent approach expands the scope of sequence-compatible strategies for stabilizing peptide folds.

Interestingly, amidines pointed inward destabilize β-sheet folding, mirroring the behavior of thioamides, which generally act as poor hydrogen-bond acceptors in sheet contexts.[11,12] However, the effects of thioamides are complicated by sulfur's hydrophobicity,[66–69] making amidines a cleaner probe of backbone hydrogen bonding.

Finally, although amidines are traditionally viewed as highly basic, this assumption arises largely from solvent-exposed benzamidine analogs.[24,60] Our spectroscopic data show that amidines embedded within peptide backbones remain largely neutral, even at pH 4. This finding calls for a reassessment of amidine basicity in structured environments and highlights opportunities for exploring new substitution patterns in peptide and peptidomimetic scaffolds.

Author contributions

B. V., E. A. O. conceived of the work. E. A. O synthesized peptides, collected and analyzed CD data. M. A. synthesized peptides and performed all experiments associated with aggregation studies. J. A. P. collected and analyzed NMR data with E. A. O. All authors contributed to the writing and proofing of the final manuscript.

Conflicts of interest

There are no conflicts to declare.

Data availability

Data for this article, including synthetic and experimental procedures, CD and NMR spectroscopic data for characterization of conformation and structure, and other supporting experiments has been included in the SI and available free of charge on the publisher's website for this article.

Experimental and spectroscopic details, CD and NMR spectra for characterization of conformational structure. See DOI: **https://doi.org/10.1039/d5sc05902j**.

Acknowledgements

The authors acknowledge the National Institutes of Health, National Institutes of General Medical Sciences under award number R35 GM142883. Additionally, we wish to thank Iowa State University Biological Nuclear Magnetic Resonance Facility (BNMRF) staff member Dr D. Bruce Fulton and Chemical Instrumentation Facility (CIF) staff members Dr Sarah Cady and Dr Kamel Harrata for instrument training pertaining to the NMR, CD, and MS results included in this publication. Research reported in this publication was supported by NIH under award number S10-OD032235 for a 700 MHz NMR upgrade, BNMRF, Iowa State University.

Notes and references

1 W. J. K. Crone, N. M. Vior, J. Santos-Aberturas, L. G. Schmitz, F. J. Leeper and A. W. Truman, *Angew. Chem., Int. Ed.*, 2016, **55**, 9639–9643.
2 K. A. Clark and M. R. Seyedsayamdost, *J. Am. Chem. Soc.*, 2022, **144**, 17876–17888.
3 A. H. Russell, N. M. Vior, E. S. Hems, R. Lacret and A. W. Truman, *Chem. Sci.*, 2021, **12**, 11769–11778.
4 N. Mahanta, D. M. Szantai-Kis, E. J. Petersson and D. A. Mitchell, *ACS Chem. Biol.*, 2019, **14**, 142–163.
5 K. L. Dunbar, H. Büttner, E. M. Molloy, M. Dell, J. Kumpfmüller and C. Hertweck, *Angew. Chem., Int. Ed.*, 2018, **130**, 14276–14280.
6 D. D. Nayak, N. Mahanta, D. A. Mitchell and W. W. Metcalf, *Elife*, 2017, **6**, e29218.
7 N. Mahanta, A. Liu, S. Dong, S. K. Nair and D. A. Mitchell, *Proc. Natl. Acad. Sci. U. S. A.*, 2018, **115**, 3030–3035.
8 A. Liu, Y. Si, S.-H. Dong, N. Mahanta, H. N. Penkala, S. K. Nair and D. A. Mitchell, *Nat. Chem. Biol.*, 2021, **17**, 585–592.

9 K. K. Sharma, K. Sharma, K. Rao, A. Sharma, G. K. Rathod, S. Aaghaz, N. Sehra, R. Parmar, B. VanVeller and R. Jain, *J. Med. Chem.*, 2024, **67**, 19932–19965.
10 M. A. McMechen, E. L. Willis, P. C. Gourville and C. Proulx, *Molecules*, 2019, **24**, year.
11 J. H. Miwa, A. K. Patel, N. Vivatrat, S. M. Popek and A. M. Meyer, *Org. Lett.*, 2001, **3**, 3373–3375.
12 K. E. Fiore, M. J. Patist, S. Giannakoulias, C.-H. Huang, H. Verma, B. Khatri, R. P. Cheng, J. Chatterjee and E. J. Petersson, *RSC Chem. Biol.*, 2022, **3**, 582–591.
13 I. J. Angera, M. M. Wright and J. R. Del Valle, *Acc. Chem. Res.*, 2024, **57**, 1287–1297.
14 E. A. O'Brien, J. A. Purslow and B. VanVeller, *Chem. Sci.*, 2024, **15**, 18992–18999.
15 S. Huh, S. D. Appavoo and A. K. Yudin, *Org. Lett.*, 2020, **22**, 9210–9214.
16 D. L. Boger, *J. Org. Chem.*, 2017, **82**, 11961–11980.
17 A. A. Aly, S. Bräse and M. A.-M. Gomaa, *Arkivoc*, 2018, **6**, 85–138.
18 A. Choudhary and R. T. Raines, *ChemBioChem*, 2011, **12**, 1801–1807.
19 Y. Luo, B. Knuckley, Y.-H. Lee, M. R. Stallcup and P. R. Thompson, *J. Am. Chem. Soc.*, 2006, **128**, 1092–1093.
20 F. Hunziker, E. Fischer and J. Schmutz, *Helv. Chim. Acta*, 1967, **50**, 1588–1599.
21 M. N. C. Soeiro, K. Werbovetz, D. W. Boykin, W. D. Wilson, M. Z. Wang and A. Hemphill, *Parasitology*, 2013, **140**, 929–951.
22 A. Lowenstern, S. M. Al-Khatib, L. Sharan, R. Chatterjee, N. M. Allen LaPointe, B. Shah, E. D. Borre, G. Raitz, A. Goode, R. Yapa, J. K. Davis, K. Lallinger, R. Schmidt, A. S. Kosinski and G. D. Sanders, *Ann. Intern. Med.*, 2018, **169**, 774–787.
23 M.-J. Wang, Y.-Q. Liu, L.-C. Chang, C.-Y. Wang, Y.-L. Zhao, X.-B. Zhao, K. Qian, X. Nan, L. Yang, X.-M. Yang, H.-Y. Hung, J.-S. Yang, D.-H. Kuo, M. Goto, S. L. Morris-Natschke, S.-L. Pan, C.-M. Teng, S.-C. Kuo, T.-S. Wu, Y.-C. Wu and K.-H. Lee, *J. Med. Chem.*, 2014, **57**, 6008–6018.
24 J. V. Greenhill and P. Lue, *Prog. Med. Chem.*, 1993, **30**, 203–326.
25 G. D. Diana, *J. Med. Chem.*, 1973, **16**, 857–859.
26 Z.-C. Wu and D. L. Boger, *Acc. Chem. Res.*, 2020, **53**, 2587–2599.
27 M. J. Moore, P. Qin, D. J. Keith, Z.-C. Wu, S. Jung, S. Chatterjee, C. Tan, S. Qu, Y. Cai, R. L. Stanfield and D. L. Boger, *J. Am. Chem. Soc.*, 2023, **145**, 12837–12852.
28 A. Okano, R. C. James, J. G. Pierce, J. Xie and D. L. Boger, *J. Am. Chem. Soc.*, 2012, **134**, 8790–8793.
29 J. Xie, A. Okano, J. G. Pierce, R. C. James, S. Stamm, C. M. Crane and D. L. Boger, *J. Am. Chem. Soc.*, 2012, **134**, 1284–1297.
30 M. J. Moore, P. Qin, D. J. Keith, Z.-C. Wu, S. Jung, S. Chatterjee, C. Tan, S. Qu, Y. Cai, R. L. Stanfield and D. L. Boger, *J. Am. Chem. Soc.*, 2023, **145**, 12837–12852.
31 C. S. Foden, S. Islam, C. Fernández-García, L. Maugeri, T. D. Sheppard and M. W. Powner, *Science*, 2020, **370**, 865–869.
32 J. Fairchild, S. Islam, J. Singh, D.-K. Bučar and M. W. Powner, *Science*, 2024, **383**, 911–918.
33 J. Singh, D. Whitaker, B. Thoma, S. Islam, C. S. Foden, A. E. Aliev, T. D. Sheppard and M. W. Powner, *J. Am. Chem. Soc.*, 2022, **144**, 10151–10155.
34 B. J. Wall, K. K. Sharma, E. A. O'Brien, A. Donovan and B. VanVeller, *J. Am. Chem. Soc.*, 2024, **146**, 11648–11656.
35 E. A. O'Brien, K. K. Sharma, J. Byerly-Duke, L. A. Camacho 3rd and B. VanVeller, *J. Am. Chem. Soc.*, 2022, **144**, 22397–22402.
36 T. S. Haque and S. H. Gellman, *J. Am. Chem. Soc.*, 1997, **119**, 2303–2304.
37 H. E. Stanger and S. H. Gellman, *J. Am. Chem. Soc.*, 1998, **120**, 4236–4237.
38 D. Eliezer, in *Characterizing Residual Structure in Disordered Protein States Using Nuclear Magnetic Resonance*, ed. Y. Bai and R. Nussinov, Humana Press, Totowa, NJ, 2006, pp. 49–67.
39 D. S. Wishart and B. D. Sykes, *J. Biomol. NMR*, 1994, **4**, 171–180.
40 Y. Wang and O. Jardetzky, *Protein Sci.*, 2002, **11**, 852–861.
41 D. Eliezer, E. Kutluay, R. Bussell Jr and G. Browne, *J. Mol. Biol.*, 2001, **307**, 1061–1073.
42 S. Spera and A. Bax, *J. Am. Chem. Soc.*, 1991, **113**, 5490–5492.
43 D. S. Wishart, B. D. Sykes and F. M. Richards, *J. Mol. Biol.*, 1991, **222**, 311–333.
44 F. A. Syud, H. E. Stanger and S. H. Gellman, *J. Am. Chem. Soc.*, 2001, **123**, 8667–8677.
45 S. R. Griffiths-Jones, A. J. Maynard and M. S. Searle, *J. Mol. Biol.*, 1999, **292**, 1051–1069.
46 M. S. Searle, S. R. Griffiths-Jones and H. Skinner-Smith, *J. Am. Chem. Soc.*, 1999, **121**, 11615–11620.
47 F. A. Syud, J. F. Espinosa and S. H. Gellman, *J. Am. Chem. Soc.*, 1999, **121**, 11577–11578.
48 S. E. Kiehna and M. L. Waters, *Protein Sci.*, 2003, **12**, 2657–2667.
49 T. Cierpicki and J. Otlewski, *J. Biomol. NMR*, 2001, **21**, 249–261.
50 G. Abrusán and J. A. Marsh, *PLoS Comput. Biol.*, 2016, **12**, e1005242.
51 S.-Y. Sheu, D.-Y. Yang, H. Selzle and E. Schlag, *Proc. Natl. Acad. Sci. U. S. A.*, 2003, **100**, 12683–12687.
52 J. Byerly-Duke, A. Donovan, E. A. O'Brien, K. K. Sharma, R. Ibrahim, L. M. Stanley and B. VanVeller, *J. Org. Chem.*, 2024, **89**, 14755–14761.
53 S. L. Deev, I. A. Khalymbadzha, T. S. Shestakova, V. N. Charushin and O. N. Chupakhin, *RSC Adv.*, 2019, **9**, 26856–26879.
54 G. Otting, B. A. Messerle and L. P. Soler, *J. Am. Chem. Soc.*, 1996, **118**, 5096–5102.
55 R. Marek, A. Lycka, E. Kolehmainen, E. Sievanen and J. Tousek, *Curr. Org. Chem.*, 2007, **11**, 1154–1205.
56 T. R. Alderson and L. E. Kay, *Curr. Opin. Struct. Biol.*, 2020, **60**, 39–49.
57 A. Fizil, Z. Gaspari, T. Barna, F. Marx and G. Batta, *Chem.–Eur. J.*, 2015, **21**, 5136–5144.

58 P. Vallurupalli, G. Bouvignies and L. E. Kay, *J. Am. Chem. Soc.*, 2012, **134**, 8148–8161.
59 N. L. Fawzi, J. Ying, R. Ghirlando, D. A. Torchia and G. M. Clore, *Nature*, 2011, **480**, 268–272.
60 P. Y. S. Lam, C. G. Clark, R. Li, D. J. P. Pinto, M. J. Orwat, R. A. Galemmo, J. M. Fevig, C. A. Teleha, R. S. Alexander, A. M. Smallwood, K. A. Rossi, M. R. Wright, S. A. Bai, K. He, J. M. Luettgen, P. C. Wong, R. M. Knabb and R. R. Wexler, *J. Med. Chem.*, 2003, **46**, 4405–4418.
61 T. M. Kamenecka, Y.-J. Park, L. S. Lin, S. de Laszlo, E. D. McCauley, G. Van Riper, L. Egger, U. Kidambi, R. A. Mumford, S. Tong, W. Tang, A. Colletti, Y. Teffera, R. Stearns, M. MacCoss, J. A. Schmidt and W. K. Hagmann, *Bioorg. Med. Chem. Lett.*, 2004, **14**, 2323–2326.
62 Y. M. Choi-Sledeski and C. G. Wermuth, *The Practice of Medicinal Chemistry (Fourth Edition)*, Academic Press, San Diego, 4th edn, 2015, pp. 657–696.
63 C. A. Fitch, G. Platzer, M. Okon, B. Garcia-Moreno E. and L. P. McIntosh, *Protein Sci.*, 2015, **24**, 752–761.
64 J. S. Richardson and D. C. Richardson, *Proc. Natl. Acad. Sci. U. S. A.*, 2002, **99**, 2754–2759.
65 B. Szała-Mendyk, T. M. Phan, P. Mohanty and J. Mittal, *Curr. Opin. Chem. Biol.*, 2023, **75**, 102333.
66 J. Byerly-Duke, E. A. O'Brien, B. J. Wall and B. VanVeller, *Methods Enzymol.*, 2024, **698**, 27–55.
67 B. J. Lampkin and B. VanVeller, *J. Org. Chem.*, 2021, **86**, 18287–18291.
68 B. Khatri, S. Raghunathan, S. Chakraborti, R. Rahisuddin, S. Kumaran, R. Tadala, P. Wagh, U. D. Priyakumar and J. Chatterjee, *Angew. Chem., Int. Ed.*, 2021, **60**, 24870–24874.
69 P. Ghosh, N. Raj, H. Verma, M. Patel, S. Chakraborti, B. Khatri, C. M. Doreswamy, S. Anandakumar, S. Seekallu, M. Dinesh, *et al.*, *Nat. Commun.*, 2023, **14**, 6050.